AMERICAN SOCIETY FOR MICROBIOLOGY | Journal of Virology®

PATHOGENESIS AND IMMUNITY

Interferon Regulatory Factor 1 Protects against Chikungunya Virus-Induced Immunopathology by Restricting Infection in Muscle Cells

Sharmila Nair,[a] Subhajit Poddar,[b] Raeann M. Shimak,[b]* Michael S. Diamond[a,b,c,d]

Departments of Medicine,[a] Pathology and Immunology,[b] and Molecular Microbiology[c] and The Andrew M. and Jane M. Bursky Center for Human Immunology and Immunotherapy Programs,[d] Washington University School of Medicine, St. Louis, Missouri, USA

ABSTRACT The innate immune system protects cells against viral pathogens in part through the autocrine and paracrine actions of alpha/beta interferon (IFN-α/β) (type I), IFN-γ (type II), and IFN-λ (type III). The transcription factor interferon regulatory factor 1 (IRF-1) has a demonstrated role in shaping innate and adaptive antiviral immunity by inducing the expression of IFN-stimulated genes (ISGs) and mediating signals downstream of IFN-γ. Although ectopic expression experiments have suggested an inhibitory function of IRF-1 against infection of alphaviruses in cell culture, its role *in vivo* remains unknown. Here, we infected *Irf1*$^{-/-}$ mice with two distantly related arthritogenic alphaviruses, chikungunya virus (CHIKV) and Ross River virus (RRV), and assessed the early antiviral functions of IRF-1 prior to induction of adaptive B and T cell responses. IRF-1 expression limited CHIKV-induced foot swelling in joint-associated tissues and prevented dissemination of CHIKV and RRV at early time points. Virological and histological analyses revealed greater infection of muscle tissues in *Irf1*$^{-/-}$ mice than in wild-type mice. The antiviral actions of IRF-1 appeared to be independent of the induction of type I IFN or the effects of type II and III IFNs but were associated with altered local proinflammatory cytokine and chemokine responses and differential infiltration of myeloid cell subsets. Collectively, our *in vivo* experiments suggest that IRF-1 restricts CHIKV and RRV infection in stromal cells, especially muscle cells, and that this controls local inflammation and joint-associated swelling.

IMPORTANCE Interferon regulatory factor 1 (IRF-1) is a transcription factor that regulates the expression of a broad range of antiviral host defense genes. In this study, using *Irf1*$^{-/-}$ mice, we investigated the role of IRF-1 in modulating pathogenesis of two related arthritogenic alphaviruses, chikungunya virus and Ross River virus. Our studies show that IRF-1 controlled alphavirus replication and swelling in joint-associated tissues within days of infection. Detailed histopathological and virological analyses revealed that IRF-1 preferentially restricted CHIKV infection in cells of nonhematopoietic lineage, including muscle cells. The antiviral actions of IRF-1 resulted in decreased local inflammatory responses in joint-associated tissues, which prevented immunopathology.

KEYWORDS interferon, interferon regulatory factor 1, interferon-stimulated genes, alphavirus, chikungunya virus, Ross River virus

Chikungunya virus (CHIKV) is transmitted to humans primarily by *Aedes aegypti* and *Aedes albopictus* mosquitoes and causes a debilitating infection characterized by fever, rash, myositis, and arthritis, with joint disease lasting for months to years in some individuals (1). While CHIKV historically caused outbreaks that were restricted to parts

Received 18 August 2017 **Accepted** 20 August 2017

Accepted manuscript posted online 23 August 2017

Citation Nair S, Poddar S, Shimak RM, Diamond MS. 2017. Interferon regulatory factor 1 protects against chikungunya virus-induced immunopathology by restricting infection in muscle cells. J Virol 91:e01419-17. https://doi.org/10.1128/JVI.01419-17.

Editor Julie K. Pfeiffer, University of Texas Southwestern Medical Center

Address correspondence to Michael S. Diamond, diamond@wusm.wustl.edu.

* Present address: Raeann M. Shimak, University of Kansas Cancer Center, Kansas City, Kansas, USA.

of Africa and Asia, an epidemic occurred in La Réunion island in 2006 (2), with subsequent spread to millions of individuals in the Indian subcontinent (3). In 2013, transmission of CHIKV occurred in the Western Hemisphere, and in 18 months, CHIKV caused more than 1.8 million cases in the Americas in more than 40 countries (4). In comparison, other arthritogenic alphaviruses (e.g., Ross River virus [RRV], Semliki Forest virus [SFV], Mayaro virus [MAYV], and Sindbis virus [SINV]) circulate with more limited global distributions.

The rapid production of interferons (IFNs) in response to a viral infection serves as a key defense mechanism in vertebrate animals (5, 6). Detection of virus occurs through the recognition of pathogen-associated molecular patterns (PAMPs) by pattern recognition receptors (PRRs), including Toll-like receptors (TLRs) and retinoic acid inducible gene 1 (RIG-I)-like receptors (RLRs). PRR engagement of single- and double-stranded viral RNA in endosomes or in the cytoplasm prompts a signaling cascade that activates and promotes nuclear translocation of IFN regulatory factor 3 (IRF-3) and NF-κB transcription factors, which bind promoter elements and induce expression of type I IFNs (7–9). After binding to their receptors, type I IFNs activate Janus kinase (JAK) and signal transducer and activator of transcription (STAT) pathways to induce expression of hundreds of IFN-stimulated genes (ISGs) with antiviral and immunomodulatory activities (10–13).

STAT1 is an essential shared component of the type I (IFN-α/β), type II (IFN-γ), and type III IFN (IFN-λ) signaling pathways, and interferon regulatory factor 1 (IRF-1) is induced by type I and type II IFNs downstream of STAT1 nuclear translocation (10). The transcription factor IRF-1 originally was identified as a regulator of IFN-β expression, due to its ability to bind IFN-stimulated regulatory elements (ISREs) present in many IFN-inducible gene promoters (14–16). IRF-1 also transduces part of the IFN-γ signal (reviewed in reference 17), as encephalomyocarditis (EMCV) virus infection in *Irf1*$^{-/-}$ fibroblasts was associated with a decrease in IFN-γ-stimulated genes, and IFN-γ-induced upregulation of cytokines and chemokines in macrophages required the transcriptional activity of IRF-1 (17–22).

IRF-1 activates antiviral programs against a diverse range of RNA viruses (23–25) and is required for inhibition of EMCV, West Nile virus (WNV), and murine norovirus (MNoV) infection in cultured cells (18, 26, 27). IRF-1 has antiviral activities that are independent of IFN signaling (28, 29), as its ectopic expression in human *STAT1*$^{-/-}$ fibroblasts inhibited infection of hepatitis C virus (HCV), yellow fever virus (YFV), WNV, CHIKV, Venezuelan equine encephalitis virus (VEEV), and human immunodeficiency virus (HIV) (25). Notwithstanding these cell-intrinsic immune activities, IRF-1 has additional functions in shaping cellular immunity. *Irf1*$^{-/-}$ mice exhibited defects in CD8$^+$ T cells and natural killer (NK) cells (30, 31) with T_H2 skewing and decreased production of IFN-γ by CD4$^+$ T cells as a consequence of a dysregulated interleukin-12 (IL-12) response (32). Whereas IRF-1 restricted WNV infection *in vivo* as a consequence of direct effects on viral replication and modulation of cellular immune responses (26), IRF-1 restricted vesicular stomatitis virus (VSV) replication in neurons in the brain through a type I and type II IFN-independent mechanism (33).

In this study, we assessed the early *in vivo* antiviral function of IRF-1 against CHIKV and RRV prior to the induction of adaptive T cell responses. *Irf1*$^{-/-}$ mice inoculated with CHIKV developed greater acute inflammation in joint-associated tissues and higher viral tissue burden at distant sites within days of infection despite having an apparently intact type I and II IFN response. Bone marrow chimera experiments and detailed immunohistochemical analysis suggest a key antiviral and anti-inflammatory role for IRF-1 in radioresistant stromal cells, including muscle cells.

RESULTS

IRF-1 controls alphavirus infection *in vivo*. To determine whether a genetic deficiency of IRF-1 affected alphavirus pathogenesis, we inoculated 4- to 5-week-old wild-type (WT) and congenic *Irf1*$^{-/-}$ C57BL/6 mice via a subcutaneous route in the footpad with 10^3 focus-forming units (FFU) of a pathogenic CHIKV (La Réunion 2006)

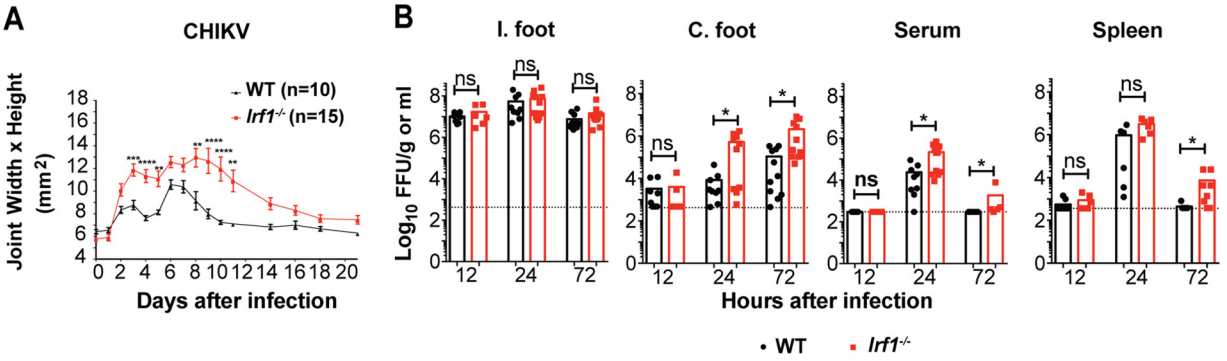

FIG 1 IRF-1 restricts arthritogenic alphaviruses *in vivo*. Four-week-old WT and *Irf1*$^{-/-}$ mice were inoculated with 10^3 FFU of CHIKV in the foot. (A) Swelling of the ipsilateral feet of infected WT ($n = 10$) and *Irf1*$^{-/-}$ ($n = 15$) mice was followed for 21 days after infection. Area was determined by measuring the width and height of the ankle region of the foot using digital calipers. Error bars represent standard error of the mean (SEM). Data are pooled from two independent experiments. Asterisks indicate statistical differences (2-way ANOVA with Sidak's multiple-comparison test: **, $P < 0.01$; ****, $P < 0.0001$). (B) Viral titers in the ipsilateral (I.) foot, contralateral (C.) foot, serum, and spleen were analyzed at 12, 24, and 72 h after infection. Data are pooled from two or three independent experiments, and each data point represents one mouse. Bars indicate mean values, and the dotted line represents the limit of detection. Asterisks indicate statistical differences (Mann-Whitney test: *, $P < 0.05$; **, $P < 0.01$; ***, $P < 0.001$).

strain and monitored foot swelling for 21 days. Compared to their WT counterparts, *Irf1*$^{-/-}$ mice were more susceptible to CHIKV-induced ipsilateral foot swelling at early (e.g., day 3) and later (e.g., day 7) time points (Fig. 1A). To begin to determine the basis for these clinical phenotypes, we measured the levels of infectious CHIKV in the joint-associated tissues, sera, and spleens of WT and *Irf1*$^{-/-}$ mice. At 12 h postinfection, no differences in viral titers were detected in any of the tissues of WT and *Irf1*$^{-/-}$ mice. Whereas the ipsilateral feet of both WT and *Irf1*$^{-/-}$ mice had similar viral burdens up to 72 h after infection, greater infection was detected in *Irf1*$^{-/-}$ mice in the contralateral feet (61-fold, $P < 0.05$) and serum (~9-fold, $P < 0.02$) at 24 h and in the contralateral feet (19-fold, $P < 0.02$), serum (7-fold, $P < 0.05$), and spleen (17-fold, $P < 0.02$) at 72 h after infection (Fig. 1B). These experiments suggest that a deficiency of IRF-1 does not substantially impact CHIKV replication at the site of inoculation but instead restricts spread at early times after inoculation.

Antiviral responses of IRF-1 and type I, type II, and type III IFNs. Since IRF-1 regulates the transcription of IFN-β and ISGs *in vitro* (25, 34), we assessed its impact on their mRNA levels in joint-associated tissues at 12 and 24 h after inoculation with CHIKV. Unexpectedly, we observed no substantive difference in expression of *Ifnβ*, *Ifnα1*, *Ifnα4*, *Ifnα13*, *Ifnα14*, *Rsad2* (viperin), *Ifit1*, or *Ifit2* mRNA in *Irf1*$^{-/-}$ and WT mice (Fig. 2A). Thus, the increased susceptibility of *Irf1*$^{-/-}$ mice to CHIKV did not appear to be due to a defect of type I IFN induction or signaling. A previous study reported a role for IRF-1 in the induction of IFN-λ expression after RLR signaling in peroxisomes (35). To test whether the increased foot swelling of *Irf1*$^{-/-}$ mice might be due to an absence of IFN-λ *in vivo*, we inoculated IFN-λ receptor knockout mice (*Ifnlr1*$^{-/-}$) with CHIKV. As no significant difference in foot swelling was observed between WT and *Ifnlr1*$^{-/-}$ mice (Fig. 2B), the effect of IRF-1 likely is not attributable to a loss of type III IFN signaling.

Since IRF-1 is induced by IFN-γ and mediates some of its antiviral effects (10), we next assessed whether the early inhibitory activity of IRF-1 against CHIKV was regulated by IFN-γ. Consistent with results of a prior study (36), we observed no differences in foot swelling and viral burden between WT and *IfngR*$^{-/-}$ mice at day 3 after infection (Fig. 2C and D). As an independent test, we inhibited IFN-γ function in both WT and *Irf1*$^{-/-}$ mice using H22, a blocking monoclonal antibody (MAb) (37). Whereas the isotype control-treated *Irf1*$^{-/-}$ mice had greater foot swelling and viral burden than their WT counterparts, as expected, we observed no effect of the IFN-γ-blocking MAb in WT or *Irf1*$^{-/-}$ mice at day 3 after infection (Fig. 2E and F). These experiments suggest that IRF-1-mediated antiviral effects against CHIKV occur independently of IFN-γ responses.

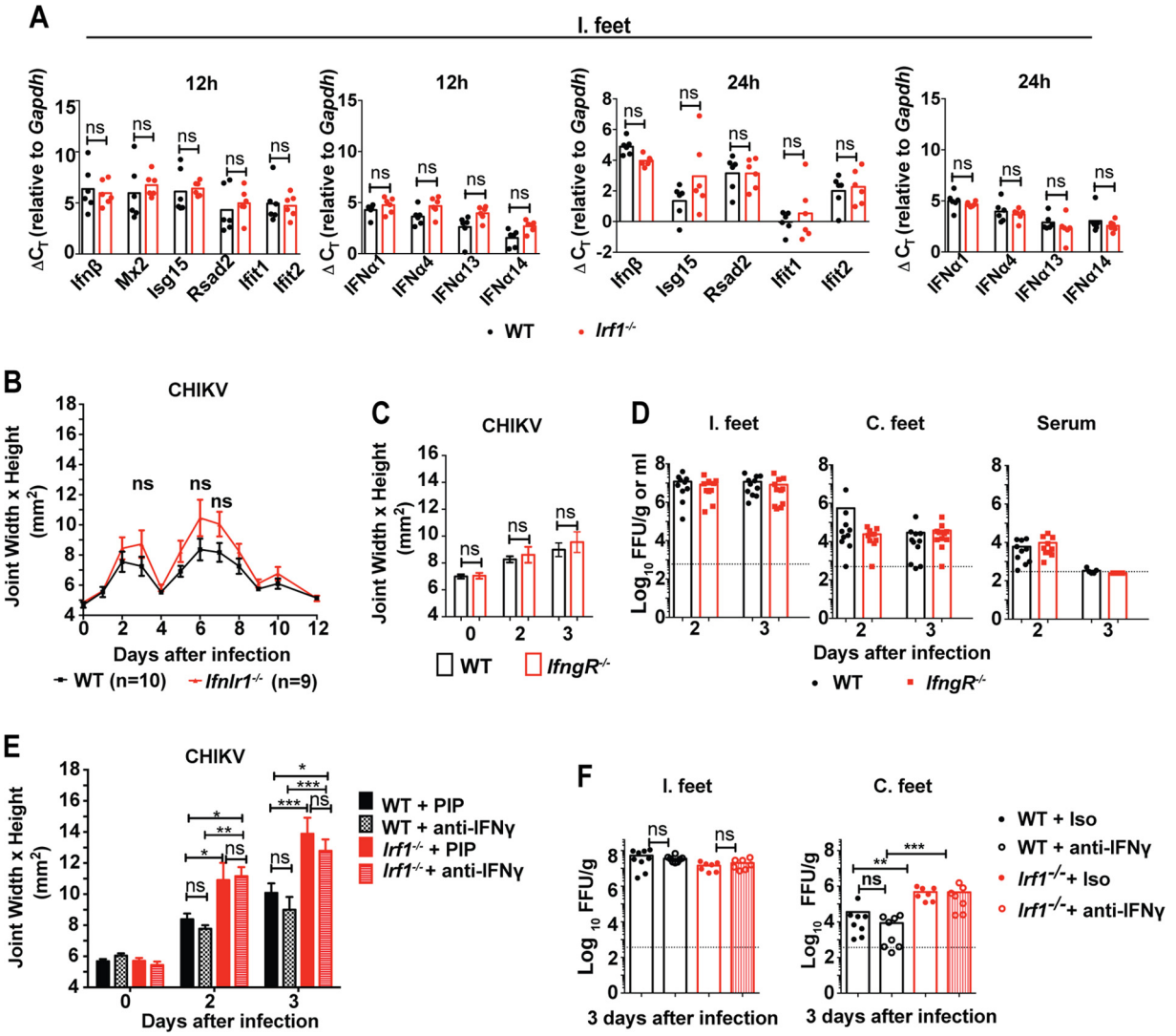

FIG 2 IRF-1-mediated antiviral responses against CHIKV are independent of IFN-α/β, IFN-λ, and IFN-γ. Four-week-old WT and *Irf1*$^{-/-}$ mice were inoculated with 10^3 FFU of CHIKV in the ipsilateral foot. (A) Ipsilateral (I.) foot joint-associated tissues were assayed for *IFN-β*, *IFN-α1*, *IFN-α4*, *IFN-α13*, *IFN-α14*, and ISGs (*Isg15*, *Rsad2*, *Ifit1*, and *Ifit2*) mRNAs by qRT-PCR. Bars indicate mean values, with each point representing one mouse from experiments performed in duplicate. Data are pooled from two independent experiments. (B) Four-week-old WT and *Ifnlr1*$^{-/-}$ mice were inoculated with 10^3 FFU of CHIKV in the foot. Swelling of the ipsilateral feet of infected WT ($n = 10$) and *Ifnlr1*$^{-/-}$ ($n = 9$) mice was followed for 12 days. Area was determined by measuring the width and height of the ankle using digital calipers. Data are pooled from two independent experiments. Error bars indicate SEM. No statistical differences were found by 2-way ANOVA with Sidak's multiple-comparison test. (C) Four-week-old WT and *IfngR*$^{-/-}$ mice were inoculated with 10^3 FFU of CHIKV in the foot. Swelling of the ipsilateral feet of infected WT ($n = 11$) and *IfngR*$^{-/-}$ ($n = 9$) mice were measured at day 2 and day 3 after infection. Error bars indicate the SEM. No statistical differences were found using a 2-way ANOVA with Sidak's multiple-comparison test. (D) Viral titers in the ipsilateral (I.) and contralateral (C.) feet were analyzed at day 3 after infection. Data are pooled from two independent experiments, and each point represents one mouse. Bars represents means, and the dotted line represents the limit of detection. No statistical difference was measured (Mann-Whitney test). (E and F) Four-week-old WT and *Irf1*$^{-/-}$ mice were treated with isotype control (PIP) or IFN-γ-blocking (H22) MAbs as indicated. (E) Swelling of the ipsilateral feet of CHIKV-infected isotype control MAb-treated WT and *Irf1*$^{-/-}$ mice (WT, days 2 and 3 [$n = 9$]; *Irf1*$^{-/-}$, day 2 [$n = 8$] and day 3 [$n = 7$]) or anti-IFN-γ-treated mice (WT, days 2 and 3 [$n = 9$]; *Irf1*$^{-/-}$, days 2 and 3 [$n = 7$]) was measured. Data are pooled from two independent experiments. Asterisks indicate statistical differences (2-way ANOVA with Sidak's multiple-comparison test: *, $P < 0.05$; **, $P < 0.01$; ***, $P < 0.001$). (F) Viral titers in the ipsilateral and contralateral feet of isotype- and anti-IFN-γ MAb-treated mice were analyzed at day 3 after infection. Data are pooled from two independent experiments, and each point represents one mouse. Bars represent mean values, and the dotted line represents the limit of detection. Asterisks indicate statistical differences (Mann-Whitney test: **, $P < 0.01$; ***, $P < 0.001$).

IRF-1-dependent antiviral responses against CHIKV preferentially occur in radioresistant cells. We next evaluated whether the antiviral actions of IRF-1 originated from the radioresistant stromal cells or radiosensitive hematopoietic cells. We established reciprocal WT and *Irf1*$^{-/-}$ chimeric mice after sublethal irradiation and bone marrow reconstitution (Fig. 3A and B). At 6 to 8 weeks after reconstitution,

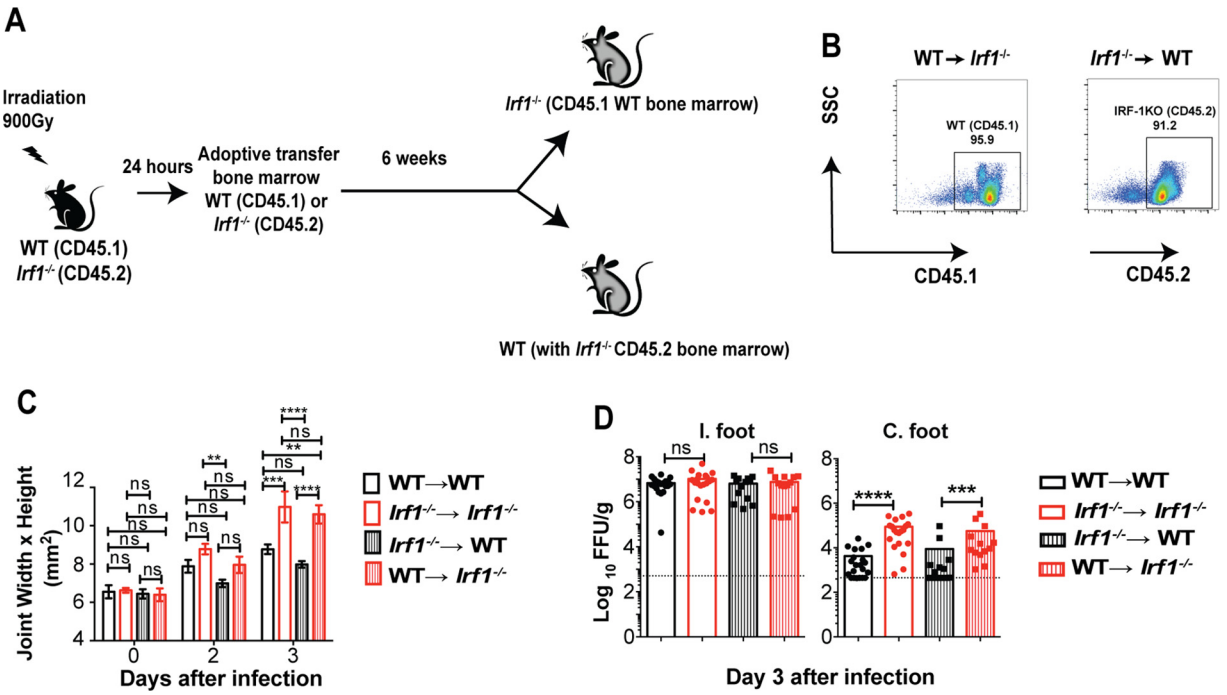

FIG 3 IRF-1 expression in radioresistant cells restricts CHIKV infection. (A) Four-week-old CD45.1$^+$ B6.SJL and CD45.2$^+$ *Irf1*$^{-/-}$ mice were irradiated and reconstituted with CD45.1$^+$ B6.SJL or CD45.2$^+$ *Irf1*$^{-/-}$ bone marrow (10^7 cells/mouse). (B) Representative flow cytometry plots of CD45.1 cells in *Irf1*$^{-/-}$ mice and CD45.2 cells in CD45.1$^+$ B6.SJL mice at 6 weeks after reconstitution. (C and D) Ten-week-old chimeric mice were inoculated with 10^3 FFU of CHIKV in the foot. (C) Swelling of the ipsilateral feet of chimeric mice WT (CD45.1) and *Irf1*$^{-/-}$ mice (WT → WT, $n = 7$; *Irf1*$^{-/-}$ → *Irf1*$^{-/-}$, $n = 8$; WT → *Irf1*$^{-/-}$, $n = 8$; *Irf1*$^{-/-}$→ WT, $n = 10$) was measured at days 0, 2, and 3 days after infection. Data are pooled from two independent experiments. Asterisks indicate statistical differences (Mann Whitney test: **, $P < 0.01$; ***, $P < 0.001$; ****, $P < 0.0001$), and error bars represent SEM. (D) Viral titers in the ipsilateral and contralateral feet of chimeric mice were analyzed at days 2 and 3 after infection. Data are pooled from two independent experiments, and each point represents one mouse. Bars represent mean values, and the dotted line represents the limit of detection. Asterisks indicate statistical differences (Mann Whitney test: ***, $P < 0.001$; ****, $P < 0.0001$).

chimeric mice were inoculated with CHIKV and monitored for foot swelling and viral infection. *Irf1*$^{-/-}$→ WT chimeras sustained foot swelling that was comparable to that of WT → WT mice (Fig. 3C). In contrast, WT → *Irf1*$^{-/-}$ chimeras had the same clinical phenotype of increased foot swelling after CHIKV infection as *Irf1*$^{-/-}$→ *Irf1*$^{-/-}$ chimeras. Virological analysis revealed that while all four groups exhibited similar titers in the ipsilateral feet, higher CHIKV infection was observed in the contralateral feet of WT → *Irf1*$^{-/-}$ and *Irf1*$^{-/-}$ → *Irf1*$^{-/-}$ mice than in those of *Irf1*$^{-/-}$ → WT and WT → WT mice (Fig. 3D). These data suggest that the antiviral effects of IRF-1 at early times after CHIKV inoculation occur largely in the radioresistant cells, and this mitigates joint-associated swelling.

Early IRF-1-dependent antiviral responses restrict CHIKV infection in muscle cells. To define the stromal cell type in which IRF-1 mediated its antiviral effects, we performed *in situ* hybridization and immunohistochemistry for viral RNA and antigen in the ipsilateral foot at day 3 after CHIKV infection of WT and *Irf1*$^{-/-}$ mice. CHIKV RNA staining in joint-associated tissues from WT and *Irf1*$^{-/-}$ mice was apparent in muscle cells and synovial fibroblasts (Fig. 4A). Corresponding hematoxylin and eosin (H&E) staining did not reveal substantive differences in leukocyte infiltration of WT and *Irf1*$^{-/-}$ joint-associated tissues at this early time point (Fig. 4B). To further assess differences in infection of WT and *Irf1*$^{-/-}$ muscle cells and fibroblasts, we costained tissue sections for CHIKV E2 antigen, skeletal muscle sarcomeric α-actinin (SAA), and fibroblast vimentin proteins. Although infected muscle cells and fibroblasts were apparent in both the ipsilateral and contralateral feet of WT and *Irf1*$^{-/-}$ mice, albeit at lower levels in the contralateral feet, we observed greater numbers of infected SAA-positive muscle cells but not vimentin-positive fibroblasts in *Irf1*$^{-/-}$ animals (Fig. 5A to C, E, and G to J). Correspondingly, higher viral titers were detected in the ipsilateral and

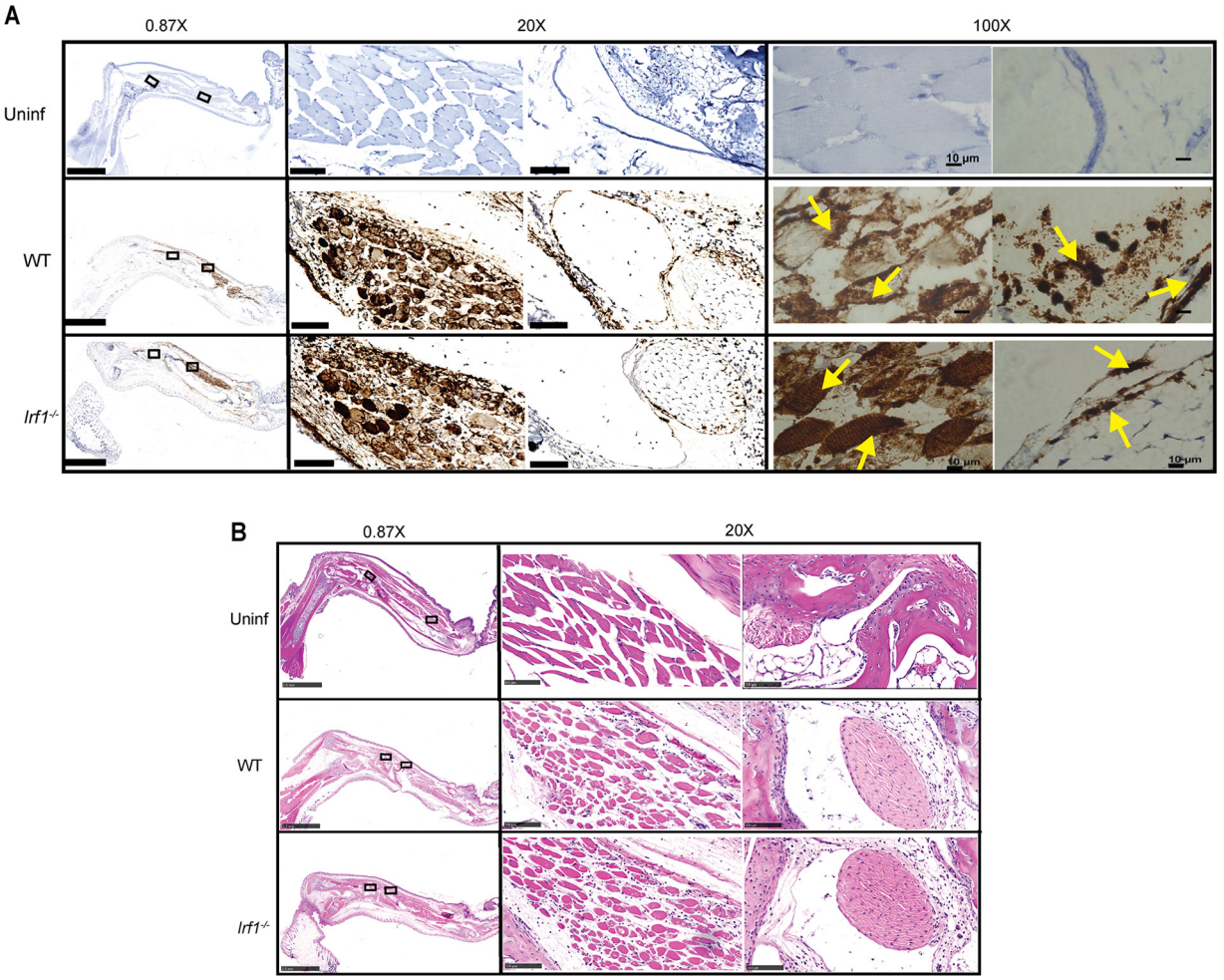

FIG 4 Loss of IRF-1 expression results in increased CHIKV infection in skeletal muscle. Four-week-old WT and *Irf1*$^{-/-}$ mice were inoculated with 10^3 FFU of CHIKV in the ipsilateral footpad, and tissues were processed on day 3 after infection. (A) *In situ* hybridization for CHIKV RNA with Gill's hematoxylin staining on naive WT and infected WT and *Irf1*$^{-/-}$ joint-associated tissues from the foot. Arrows on the 100× images indicate CHIKV RNA (brown staining) in muscle and fibroblast cells. Cell types were distinguished by morphology. (B) Hematoxylin and eosin staining of CHIKV-infected WT and *Irf1*$^{-/-}$ joint-associated tissues. Scale bars at magnification: 0.87× = 2.5 mm, 20× = 100 μm, and 100× = 10 μm. The 0.87× and 20× images were acquired on a Hamamatsu NanoZoomer 2.0-HT system. The 100× images were acquired on a Zeiss Axio Obesrver.D1 Widefield fluorescence microscope. Data are representative of at least two independent experiments with two mice per experiment.

contralateral gastrocnemius muscles from *Irf1*$^{-/-}$ mice than in those from WT mice at 24 and 72 h after infection (Fig. 5D and F). These data suggest that IRF-1-dependent antiviral responses preferentially restrict CHIKV replication in skeletal muscle cells during the early stages of infection.

Impact of IRF-1 on inflammatory responses. To determine whether the enhanced swelling observed in the extremities of CHIKV-infected *Irf1*$^{-/-}$ mice at day 3 was due to an altered inflammatory response, we determined the composition of the cell infiltrates using flow cytometry (Fig. 6A). Consistent with the histological analysis of tissue sections (Fig. 4B), the total numbers of CD45$^+$ leukocytes in the feet were similar for WT and *Irf1*$^{-/-}$ mice at day 3 after infection. However, an analysis of immune cell types revealed that CHIKV-infected *Irf1*$^{-/-}$ mice had greater infiltration of granulocytes (CD11b$^+$ Ly6G^{hi} Ly6C^{mid} neutrophils [5.4-fold, $P < 0.0001$] and CD11b$^+$ SiglecF$^+$ eosinophils [3.2-fold, $P < 0.005$]) but fewer CD11b$^+$ Ly6C^{hi} inflammatory monocytes (1.6-fold, $P < 0.05$) in their ipsilateral feet than WT mice (Fig. 6A). Given the differences in myeloid cell trafficking patterns, we measured a panel of 24 cytokines and chemokines in the soft tissues of the ipsilateral foot at day 3. We detected higher expression of IL-4, IL-6, CXCL1, CXCL2, CCL3, and CCL4 in CHIKV-infected *Irf1*$^{-/-}$ mice than in WT

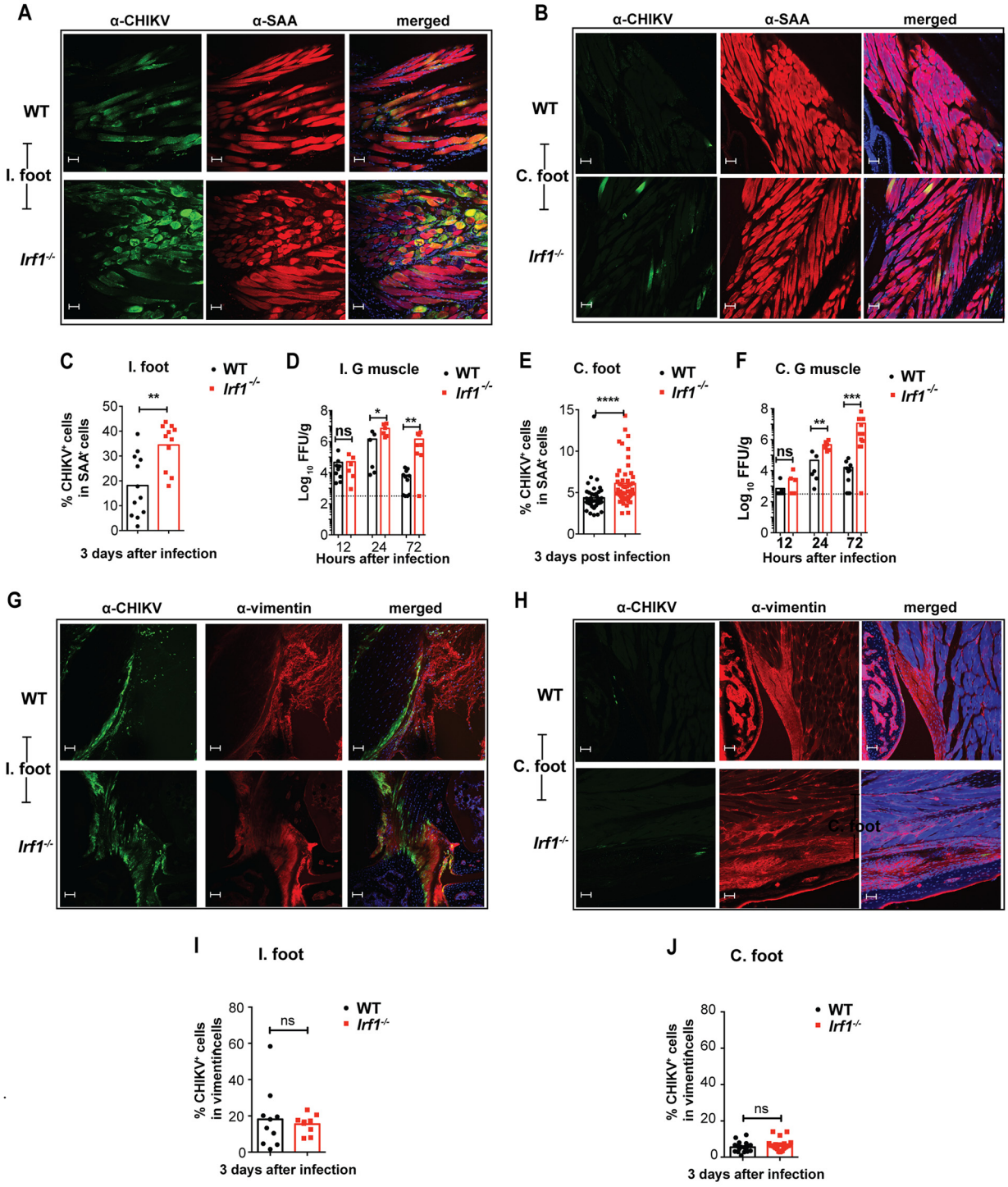

FIG 5 Loss of IRF-1 expression results in increased CHIKV antigen and infection in skeletal muscle. (A to C, E, and G to J) Confocal microscopy analysis of ipsilateral (I.) and contralateral (C.) joint-associated tissues at day 3 after CHIKV inoculation of WT and *Irf1*$^{-/-}$ mice. The sections were stained for CHIKV E2 antigen using anti-CHIKV MAbs (CHK-152 and CHK-166). The sections were counterstained with DAPI and costained with anti-sarcomeric α-actinin (SAA) (A and B) or anti-vimentin (G and H). Scale bars, 50 μm. CHIKV antigen colocalization in SAA-positive muscle cells of ipsilateral (C) and contralateral (E) feet or in vimentin-positive fibroblasts of ipsilateral (I) and contralateral (J) feet was quantified using Image J software. Data are pooled from two or three independent experiments with 1 or 2 mice in each experiment (2 to 4 sections per mouse). Bars represent mean values, and each data point represents the percentage of colocalization from each quantified image. Asterisks indicate statistical significance (Mann Whitney test: **, $P < 0.01$). (D and F) Viral titers in the ipsilateral (I.) (D) and contralateral (C.) (F) gastrocnemius muscles at 12, 24, and 72 h after infection. Data are pooled from three independent experiments, and each point represents one mouse. Bars indicate mean values, and the dotted line represents the limit of detection. Asterisks indicate statistical differences (Mann-Whitney test: *, $P < 0.05$; **, $P < 0.01$; ***, $P < 0.001$)

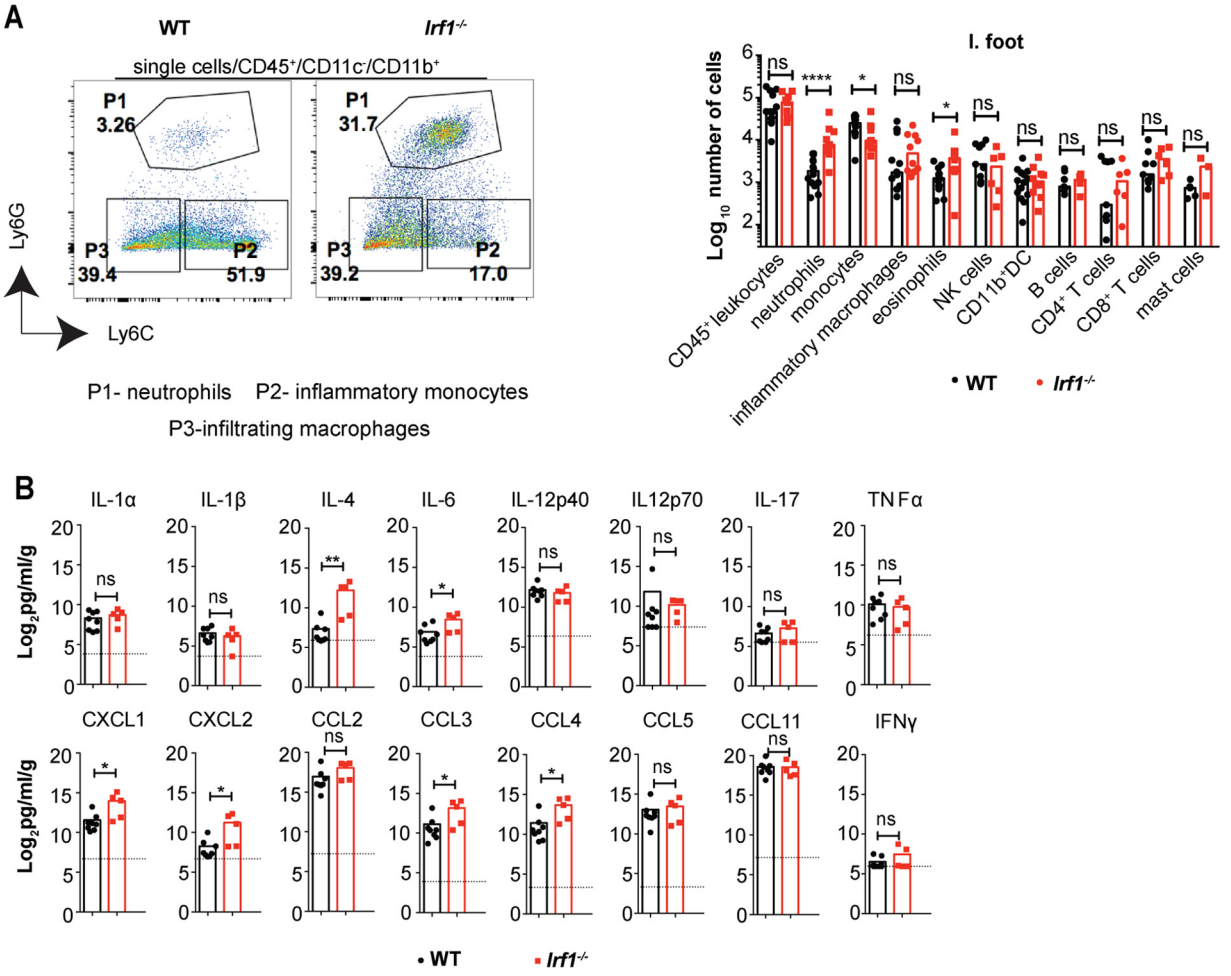

FIG 6 Loss of IRF-1 results alters inflammatory responses in infected tissue. (A) Representative flow cytometry plots for neutrophils ($CD11c^-$ $CD11b^+$ $Ly6G^{hi}$ $Ly6C^{mid}$), inflammatory monocytes ($CD11c^-$ $CD11b^+$ $Ly6G^-$ $Ly6C^{hi}$), and macrophages ($CD11c^-$ $CD11b^+$ $Ly6G^-$ $Ly6C^-$) in the ipsilateral feet of CHIKV-infected WT mice at day 3 after infection (left) and numbers of immune cells subsets in the ipsilateral feet of CHIKV-infected WT and *Irf1*$^{-/-}$ mice (right). Data are pooled from three independent experiments, with each dot representing an individual mouse. Bars indicate mean values, and asterisks denote statistical differences (Mann-Whitney test: *, $P < 0.05$; **, $P < 0.01$; ****, $P < 0.0001$; ns, not significant). (B) The joint-associated tissues from the ipsilateral feet were harvested at day 3 and analyzed for proinflammatory cytokines and chemokines. Bars indicate mean values, dotted lines represent the limit of detection, and each point represents one mouse. Values below the limit of detection were plotted at the limit of detection. Data are pooled from two independent experiments. Asterisks indicate statistical differences (Mann-Whitney test: *, $P < 0.05$; **, $P < 0.01$; ns, not significant).

mice (Fig. 6B). However, no significant differences in levels of cytokines IL-1α, IL-1β, IL-12p40, IL-12p70, IL-17, tumor necrosis factor alpha (TNF-α), and IFN-γ and chemokines CCL2, CCL5, and CCL11 were observed between WT and *Irf1*$^{-/-}$ mice. (Fig. 2A). The remaining eight cytokines (IL-2, IL-3, IL-5, IL-9, IL-10, IL-13, IL-17A, and granulocyte-macrophage colony-stimulating factor [GM-CSF]) were below the level of detection at day 3 after infection. The increased expression of granulocyte-attracting chemokines (e.g., CXCL1, CXCL2, and CCL3) in joint-associated tissues from *Irf1*$^{-/-}$ mice may explain the greater influx of neutrophils and eosinophils after CHIKV infection. Thus, IRF-1 expression in joint-associated tissues early during infection regulates the local inflammatory responses, possibly because of its ability to control CHIKV replication in specific cell types.

Early IRF-1-dependent antiviral responses also restrict RRV infection. To test whether the antiviral effect of IRF-1 could affect replication of another arthritogenic alphavirus, we inoculated WT and *Irf1*$^{-/-}$ mice via a subcutaneous route with RRV and evaluated the viral burden in the ipsilateral foot and at distant sites. Immunohistochemical analysis revealed greater numbers of RRV-infected muscle cells in *Irf1*$^{-/-}$ than

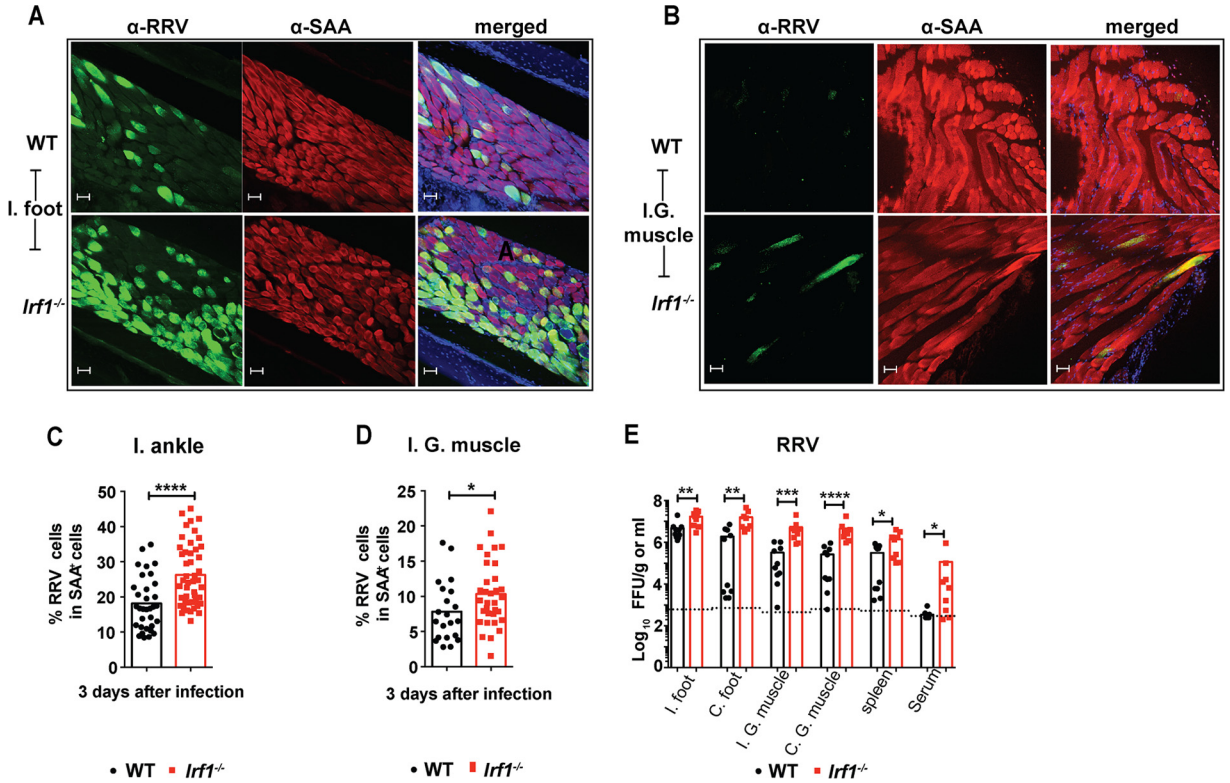

FIG 7 Loss of IRF-1 expression results in increased RRV infection. Four-week-old WT and *Irf1*$^{-/-}$ mice were inoculated with 10^3 FFU of RRV in the footpad. (A and B) Confocal microscopy analysis of ipsilateral (I.) feet (A) and ipsilateral gastrocnemius (I.G.) muscles (B) at day 3 after RRV infection of WT and *Irf1*$^{-/-}$ mice. The sections were stained for E2 antigen using anti-RRV MAbs. The sections were counterstained with DAPI and costained with anti-sarcomeric α-actinin (SAA). Scale bars, 50 μm. (C and D) Quantification of RRV E2 antigen colocalization in SAA-positive muscle cells of ipsilateral (I.) feet (C) and ipsilateral gastrocnemius (I.G.) muscles (D) from WT and *Irf1*$^{-/-}$ mice. Data are pooled from 3 mice (3 or 4 sections per mouse). Bars indicate mean values, and each data point represents the percentage of colocalization of RRV antigen in SAA-positive cells from each image. Asterisks indicate statistical significance (Mann-Whitney test: ****, $P < 0.0001$; *, $P < 0.05$). (E) Infectious viral burden was measured in the ipsilateral (I.) and contralateral (C.) feet, quadriceps muscle, spleen, and serum at day 3 after infection. Data are pooled from two independent experiments, and each point represents one mouse. Bars indicate mean values, and the dotted line represents the limit of detection Asterisks indicate statistical differences (Mann-Whitney test: *, $P < 0.05$; **, $P < 0.01$; ***, $P < 0.001$; ****, $P < 0.0001$).

in WT mice (Fig. 7A to D). Since RRV infection does not cause clinical signs in mice within the first 4 days of infection (38), we measured viral titers at day 3. Higher RRV titers were measured in the ipsilateral (4-fold, $P = 0.002$) and contralateral (8-fold, $P < 0.002$) feet, ipsilateral (16-fold, $P = 0.002$) and contralateral (18-fold, $P < 0.0001$) quadriceps muscles, sera (650-fold, $P < 0.005$), and spleens (4-fold, $P < 0.05$) of *Irf1*$^{-/-}$ than in those of WT mice (Fig. 7C). Thus, IRF-1 has an early antiviral function against infection by multiple arthritogenic alphaviruses.

DISCUSSION

Although the roles of IRF-3, IRF-7, and IRF-9 in regulating IFN-dependent defense responses are established, the biological relevance of the transcription factor IRF-1 in antiviral responses has remained less certain despite its discovery more than 20 years ago (34). IRF-1-mediated antiviral responses have been reported *in vitro* against a range of viruses, including WNV, tick borne encephalitis virus, YFV, HCV, EMCV, MNoV, and VSV (18, 26, 27, 29, 33, 39, 40). Although *in vivo* studies in mice have established a protective role for IRF-1 against WNV, MNoV, and VSV (26, 27, 33), the contribution of its innate functions has remained less certain. Indeed, in the sole prior study with *Irf1*$^{-/-}$ mice and an alphavirus (VEEV), only the effects of IRF-1 on vaccine immunity were explored (41). We evaluated the effects of IRF-1 on the early (day 3 and prior) antiviral responses against arthritogenic alphaviruses *in vivo* prior to induction of adaptive immunity. We identified IRF-1 as an essential component of the early host immune response against CHIKV and RRV. *Irf1*$^{-/-}$ mice were more susceptible to

infection at early time points, and in the context of CHIKV infection they developed enhanced musculoskeletal disease characterized by increased foot swelling. As we assessed the antiviral function of IRF-1 prior to its well-characterized effects on maturation of adaptive T cell responses (26, 32), the effects of IRF-1 on early CHIKV pathogenesis preferentially reflect its innate immune activity.

Type I, II, and III IFNs are mediators of the early innate immune response by virtue of their ability to induce panoply of ISGs with antiviral and proinflammatory activities, the latter of which shape the cellularity of infiltrating immune responses (reviewed in references 5, 10, 17, 42, 43, 44, and 35). Unexpectedly, type I IFN signaling functions appeared to be intact in joint-associated tissues in *Irf1*$^{-/-}$ mice, as IFN-α, IFN-β, and ISG mRNA expression levels were not altered after CHIKV infection compared to those in WT mice. Thus, the increased swelling and virological phenotypes in CHIKV-infected *Irf1*$^{-/-}$ mice were not due to altered type I, II, or III IFN signaling pathways. At least in the context of CHIKV infection, IRF-1-dependent transcriptional signals appear to activate antiviral effector pathways directly to achieve host-mediated control.

Alphaviruses have evolved strategies to evade cell-intrinsic and -extrinsic innate host defenses, including host translational shutoff (45), blockade of transcription of IRF-3-dependent antiviral genes (46), and direct evasion of antiviral ISGs (47). Despite the many ways that alphaviruses antagonize antiviral defenses, host cells still restrict their infection. Indeed, IRF-1 can mediate antiviral effects in the absence of IFNs (48) by binding to conserved elements in the promoters of its target genes. Even in STAT1$^{-/-}$ cells, which lack efficient type I, II, or III IFN signaling, ectopic expression of IRF-1 induced more than 100 target genes and inhibited replication of several families of viruses, including alphaviruses (25, 40). Consistent with these data, ectopic expression of IRF-1 in cortical neurons inhibited infection of flaviviruses (WNV and St. Louis encephalitis viruses), alphaviruses (VEEV), and coronaviruses (mouse hepatitis virus) (49), and *in vivo*, IRF-1 expression reduced infection by VSV in neurons through a type I-independent mechanism (33). At present, it remains unknown which IRF-1-induced genes mediate the antiviral effects against alphaviruses or other unrelated viral families.

Since the epidemic in La Réunion Island of 2006 and its spread to the Western Hemisphere, the mechanisms of immune-mediated protection and pathogenesis of CHIKV infection and disease have been studied intensively (50). Experimental infection of different strains of immunocompetent mice results in an acute and persistent musculoskeletal disease characterized by infection and inflammation of joint-associated tissues, resulting in myositis, synovitis, and, arthritis (51–54). In terms of the cellular tropism in musculoskeletal tissues, in mice and nonhuman primates, CHIKV replicates preferentially in fibroblasts, mesenchymal cells, and osteoblasts (55, 56). CHIKV infection in humans commonly causes myositis (57); indeed, in the La Réunion island outbreak 97.7% of individuals reported muscle pain (58), and biopsies of CHIKV-infected individuals revealed CHIKV antigen in muscle satellite cells (59). In our murine model of CHIKV infection, IRF-1 expression in radioresistant stromal cells mitigated infection and swelling of joint-associated tissues. Our virological and immunohistochemical studies suggest that IRF-1-dependent antiviral responses in muscle cells contribute to restriction of infection *in vivo*.

Local inflammatory responses in joint-associated tissues influence disease progression during arthritogenic alphavirus infections (38, 51, 53). Studies in mice have shown that a dysregulated myeloid cell response promotes joint swelling and immune-mediated pathology (60, 61). Our studies establish a key role of IRF-1 in preventing excessive musculoskeletal disease by restricting virus replication in muscle cells and thus dampening expression of proinflammatory cytokines and chemokines. DD264 and brequinar are broad-spectrum antiviral compounds that have activity against CHIKV and reportedly function through an IRF-1-dependent cell-intrinsic immune amplification (62). As DD264 becomes commercially available, the specificity of its mechanism of action can be corroborated in CHIKV-infected WT and *Irf1*$^{-/-}$ mice. Given the reported toxic effects of brequinar on myeloid cells (63, 64), interpretation of results after *in vivo* administration of this drug may be more challenging.

In summary, our experiments establish that IRF-1 is a key transcription factor in the host defense response against arthritogenic alphavirus infection. Because IRF-1 can regulate antiviral genes directly in a cell type-specific and IFN-independent manner (40), evaluations of candidate downstream effector genes through clustered regularly interspaced short palindromic repeat (CRISPR)-Cas9 gene editing are planned. Moreover, when *Irf1*$^{fl/fl}$ mice become available, conditional gene deletion in muscle cells and/or fibroblasts *in vivo* will further delineate the temporal and spatial roles of IRF-1 in regulating alphavirus tropism and inflammation in joint-associated tissues. Such studies might identify genes that can be targeted pharmacologically to minimize alphavirus infection and disease in key cell types.

MATERIALS AND METHODS

Virus propagation and titration. CHIKV (La Reunion OPY1 p142, 2006) and RRV (T48) were the gifts of S. Higgs (Kansas State University) and R. Kuhn (Purdue University), respectively; they were produced from infectious cDNA clones according to established protocols (38, 65) and propagated in C6/36 *Aedes albopictus* cells. Vero cells were used for titration in a virus focus-forming assay (FFA) as described previously (66).

Mouse experiments and tissue preparation. This study was carried out in accordance with the recommendations in the *Guide for the Care and Use of Laboratory Animals* of the National Institutes of Health. The protocols were approved by the Institutional Animal Care and Use Committee at the Washington University School of Medicine (assurance number A3381-01). Virus inoculations were performed under anesthesia induced and maintained with ketamine hydrochloride and xylazine, and all efforts were made to minimize animal suffering. All mouse infection studies were performed in an animal biosafety level 3 (A-BSL3) laboratory.

Wild-type (WT) C57BL/6J (CD45.2, strain 000664) and B6-SJL (CD45.1, strain 002014) mice were purchased from Jackson Laboratories. Congenic, backcrossed *Irf1*$^{-/-}$ (31, 67), *IFNgR*$^{-/-}$ (42) and *Ifnlr1*$^{-/-}$ (43, 44) mice were obtained from T. Taniguchi (Tokyo, Japan), H. Virgin (St. Louis, MO), and S. Doyle (Seattle, WA), respectively, and then genotyped and bred in the animal facility of Washington University School of Medicine. For infection, 4-week-old (unless mentioned otherwise) age-matched male and female mice were used. Mice were inoculated subcutaneously in the footpad (10^3 focus-forming units [FFU] in 10 μl) with virus diluted in phosphate-buffered saline (PBS). Foot size and swelling were measured prior to infection and monitored daily with digital calipers (Fowler, 100 mm digital caliper). To quantitate viral burden in tissues on specific days after infection, mice were perfused extensively with PBS, tissues were harvested and weighed, and virus titers were determined by focus forming assay (FFA) as described previously (66).

qRT-PCR assay. Mouse organs were homogenized in TRIzol reagent (Invitrogen). Total RNA was isolated after TRIzol-chloroform extraction, and quantitative reverse transcription-PCR (qRT-PCR) was performed using the One-Step RT-PCR master mix and a 7500 Fast real-time PCR system (Applied Biosystems). *IFNβ*, *Ifnα1*, *Ifnα4*, *Ifnα13*, *Ifnα14*, *Ifit2*, *Ifit1*, *Rsad2*, and *ISG15* were detected using qRT-PCR and normalized to *Gapdh* expression using the following PrimeTime assays (IDT) according to the manufacturer's instructions. *IFNβ*, Mm.PT.58.30132453; *IFNα1*, Mm.PT.58.43426930; *IFNα4*, Mm.PT.58.7678281; *IFNα13*, Mm.PT.58.41423993; *IFNα14*, Mm.PT.58.42242727; *Ifit1*, Mm.PT.58.32674307; *Ifit2*, Mm.PT.58.28800045.g; *Rsad2*, mm.PT.58.11280480; *Isg15*, mm.PT.58.41476392.g; and *Gapdh*, Mm.PT.39a1.

Cytokine and chemokine analysis. Mice were inoculated subcutaneously with 10^3 FFU of CHIKV in the footpad, and the ipsilateral foot was collected at 3 days after infection, homogenized, and analyzed for cytokines and chemokines using a Bio-Plex Pro mouse cytokine 23-plex assay kit (Bio-Rad) and a mouse MIP2/CXCL2 Quantikine enzyme-linked immunosorbent assay (ELISA) kit (R&D Systems) according to the manufacturer's instructions.

IFN-γ neutralization. Four-week-old WT and *Irf1*$^{-/-}$ mice were inoculated with 10^3 FFU of CHIKV and at 1 day postinfection were administered an anti-IFN-γ blocking monoclonal antibody (MAb H22; Leinco, I-438) or an IgG isotype control antibody (MAb PIP; Leinco, I-140). Foot swelling and virological titers were analyzed at day 2 and/or day 3 after infection.

Bone marrow chimeras. Chimeric mice were generated by using modifications to a published protocol (68). Briefly, 4-week-old WT and *Irf1*$^{-/-}$ mice were irradiated with 900 Rads and reconstituted via intravenous injection with 10^7 bone marrow cells isolated from the tibias and femurs of 4- to 5-week-old *Irf1*$^{-/-}$ (CD45.2) or WT (CD45.1) mice. At 6 to 8 weeks after bone marrow transplantation, *Irf1*$^{-/-}$ (CD45.2) → WT (CD45.1) and WT (CD45.1) → *Irf1*$^{-/-}$ mice were bled to confirm chimerism by flow cytometry. Mice were inoculated with 10^3 FFU of CHIKV via a subcutaneous route. Foot swelling and viral burden in joints were monitored.

Flow cytometry. Chimeric mice were bled, and peripheral blood mononuclear cells were collected. Cells were stained with CD45.1 V500 (BioLegend, 110741) or CD45.2 allophycocyanin (APC) (eBioscience, 56-0454-82) and analyzed on a MACS Quant Analyzer10 flow cytometer (Miltenyi). Flow cytometry also was performed on joint-associated tissues from WT and *Irf1*$^{-/-}$ mice at day 3 after CHIKV infection. After extensive cardiac perfusion, the ipsilateral feet were skinned and disjointed from the tibia. The feet were digested with collagenase-DNase I solution (2.5 mg/ml collagenase [Sigma, C-0130] and DNase I [Sigma, D5025] in RPMI with 10% fetal bovine serum [FBS] [HyClone]) for 2 h at 37°C with constant agitation. Cells were separated by centrifugation and stained with antibodies to CD45 AF700 (BioLegend, 103128), CD11c APC-Cy7 (BioLegend, 117324), SiglecF phycoerythrin (PE) (BD, 552128), Ly6G PE-Cy7 (BioLegend,

127618), Ly6C Pacific Blue (BioLegend, 128014), CD3 Pacific Blue (BioLegend, 100214), CD4 APC (BioLegend, 100516), CD8 PE-Cy7 (BioLegend, 100722), B220 V500 (BioLegend, 103227), NK1.1 fluorescein isothiocyanate (FITC) (BioLegend, 108706), c-kit APC (BioLegend, 105812), and CD11b peridinin chlorophyll protein (PerCP)-Cy5.5 (BioLegend, 101228). Cells were analyzed by multicolor flow cytometry on a BD Fortessa. All data were processed using FlowJo software (FlowJo, LLC).

Immunohistochemistry. Immunohistochemical staining was performed on CHIKV- or RRV-infected WT and *Irf1*$^{-/-}$ mice at 3 days after infection. After extensive cardiac perfusion with PBS followed by 4% paraformaldehyde (PFA), the ipsilateral and contralateral feet and gastrocnemius muscle were collected and fixed for 24 h in 4% PFA. Some of the fixed tissues were decalcified (with 14% EDTA titrated to pH 7.2 with ammonium hydroxide) for 5 to 7 days. Tissues then were washed in PBS, incubated in 30% sucrose in 0.1 M phosphate buffer for an additional 24 h, and frozen in Tissue Tek compound (Sakura, 4583) at −80°C. Sagittal slices (30 μm) were cut using a cryostat (Microm, HM505N), and all staining procedures were performed as free floating. Following a 1-h blocking step at room temperature in PBS supplemented with 1% bovine serum albumin (BSA), 0.2% Triton, and 10% goat serum, the sections were incubated overnight at 4°C in primary antibody solutions containing 10% goat serum and 0.2% Triton in PBS. The following antibodies were used: monoclonal humanized anti-CHIKV (CHK-166 and CHK-152 [66]; 2 μg/ml each), monoclonal human anti-RRV (RRV-1I9 [69] and/or RRV-86 [gift of J. Crowe, Vanderbilt University]; 2 μg/ml each), polyclonal rabbit antivimentin (Abcam, ab8978; dilution, 1:300), and polyclonal rabbit anti-sarcomeric α-actinin (Abcam, ab137346; dilution, 1:100). Secondary anti-mouse Alexa Fluor 555 and/or anti-rabbit Alexa Fluor 488 (Invitrogen) was incubated 1:500 in PBS for 2 h at room temperature, and nuclei were visualized with DAPI (4′,6-diamidino-2-phenylindole). Slides were mounted with Vectashield mounting medium (Vector Laboratories). Tissues were imaged on a Zeiss LSM880 confocal microscope at the Washington University Microscopy Core Facility. Image analysis and quantification of virus-infected SAA-positive or vimentin-positive cells were performed blinded to the investigator, using ImageJ software.

Viral RNA *in situ* hybridization. RNA *in situ* hybridization was performed using RNAscope 2.5 (Advanced Cell Diagnostics) according to the manufacturer's instructions. PFA-fixed, decalcified, and paraffin-embedded tissue sections were deparaffinized by incubating for 60 min at 60°C. Endogenous peroxidases were quenched with H_2O_2 for 10 min at room temperature. Slides were boiled for 15 min in RNAscope target retrieval reagents and incubated for 30 min in RNAscope Protease Plus before probe hybridization. The probe targeting CHIKV RNA (479501) was designed and synthesized by Advanced Cell Diagnostics. Tissues were counterstained with Gill's hematoxylin and visualized using the Hamamatsu NanoZoomer 2.0-HT system. Images were acquired on a Zeiss Axio Obesrver.D1 Widefield fluorescence microscope at the Washington University Microscopy Core Facility.

Statistical analysis. All data were analyzed using Prism software (GraphPad6, San Diego, CA). Measurements of foot swelling were analyzed by 2-way analysis of variance (ANOVA) with Sidak's multiple comparison tests unless mentioned otherwise. Virological analyses of tissues, cytokine and chemokine measurements, flow cytometry data, and immunohistochemical quantification all were analyzed with the Mann-Whitney test.

ACKNOWLEDGMENTS

National Institutes of Health grants R01 AI073755, R01 AI104972, and R01 AI114816 and the NIH Shared Instrumentation Grant (S10 RR027552) for the Hamamatsu NanoZoomer 2.0-HT System supported this study. S. Nair was supported by the Deutsche Forschungsgemeinschaft.

We thank H. Lazear and H. Lin for help with data collection from CHIKV-infected *Ifnlr1*$^{-/-}$ mice, M. Noll for technical assistance with animal husbandry, the Digestive Diseases Research Cores Center (DDRCC) core at Washington University at St. Louis for processing of tissues, W. Beatty and B. Anthony at the Molecular Microbiology Imaging facility for assistance with confocal microscopy, J. Crowe (Vanderbilt University) for antibodies, and S. Doyle (ZymoGenetics) for providing the *Ifnlr1*$^{-/-}$ mice.

REFERENCES

1. Schilte C, Staikowsky F, Couderc T, Madec Y, Carpentier F, Kassab S, Albert ML, Lecuit M, Michault A. 2013. Chikungunya virus-associated long-term arthralgia: a 36-month prospective longitudinal study. PLoS Negl Trop Dis 7:e2137. https://doi.org/10.1371/journal.pntd.0002137.
2. Paganin F, Borgherini G, Staikowsky F, Arvin-Berod C, Poubeau P. 2006. Chikungunya on Reunion Island: chronicle of an epidemic foretold. Presse Med 35:641–646. https://doi.org/10.1016/S0755-4982(06)74657-7.
3. Sissoko D, Malvy D, Ezzedine K, Renault P, Moscetti F, Ledrans M, Pierre V. 2009. Post-epidemic Chikungunya disease on Reunion Island: course of rheumatic manifestations and associated factors over a 15-month period. PLoS Negl Trop Dis 3:e389. https://doi.org/10.1371/journal.pntd.0000389.
4. PAHO. Chikungunya: PAHO/WHO data, maps, and statistics. http://www.paho.org/hq/index.php?option=com_topics&view=rdmore&cid=8379&Itemid=40931.
5. Koyama S, Ishii KJ, Coban C, Akira S. 2008. Innate immune response to viral infection. Cytokine 43:336–341. https://doi.org/10.1016/j.cyto.2008.07.009.
6. Zhou H, Chen S, Wang M, Cheng A. 2014. Interferons and their receptors in birds: a comparison of gene structure, phylogenetic analysis, and cross modulation. Int J Mol Sci 15:21045–21068. https://doi.org/10.3390/ijms151121045.
7. Kumagai Y, Takeuchi O, Akira S. 2008. Pathogen recognition by innate receptors. J Infect Chemother 14:86–92. https://doi.org/10.1007/s10156-008-0596-1.

8. Takeuchi O, Akira S. 2008. MDA5/RIG-I and virus recognition. Curr Opin Immunol 20:17–22. https://doi.org/10.1016/j.coi.2008.01.002.
9. Takeuchi O, Akira S. 2007. Recognition of viruses by innate immunity. Immunol Rev 220:214–224. https://doi.org/10.1111/j.1600-065X.2007.00562.x.
10. Boehm U, Klamp T, Groot M, Howard JC. 1997. Cellular responses to interferon-gamma. Annu Rev Immunol 15:749–795. https://doi.org/10.1146/annurev.immunol.15.1.749.
11. Meraz MA, White JM, Sheehan KC, Bach EA, Rodig SJ, Dighe AS, Kaplan DH, Riley JK, Greenlund AC, Campbell D, Carver-Moore K, DuBois RN, Clark R, Aguet M, Schreiber RD. 1996. Targeted disruption of the Stat1 gene in mice reveals unexpected physiologic specificity in the JAK-STAT signaling pathway. Cell 84:431–442. https://doi.org/10.1016/S0092-8674(00)81288-X.
12. Lackmann M, Harpur AG, Oates AC, Mann RJ, Gabriel A, Meutermans W, Alewood PF, Kerr IM, Stark GR, Wilks AF. 1998. Biomolecular interaction analysis of IFN gamma-induced signaling events in whole-cell lysates: prevalence of latent STAT1 in high-molecular weight complexes. Growth Factors 16:39–51. https://doi.org/10.3109/08977199809017490.
13. de Veer MJ, Holko M, Frevel M, Walker E, Der S, Paranjape JM, Silverman RH, Williams BR. 2001. Functional classification of interferon-stimulated genes identified using microarrays. J Leukoc Biol 69:912–920.
14. Kamijo R, Harada H, Matsuyama T, Bosland M, Gerecitano J, Shapiro D, Le J, Koh SI, Kimura T, Green SJ, Mak TW, Taniguchi T, Villek J. 1994. Requirement for transcription factor IRF-1 in NO synthase induction in macrophages. Science 263:1612–1615. https://doi.org/10.1126/science.7510419.
15. Pine R, Decker T, Kessler DS, Levy DE, Darnell JE, Jr. 1990. Purification and cloning of interferon-stimulated gene factor 2 (ISGF2): ISGF2 (IRF-1) can bind to the promoters of both beta interferon- and interferon-stimulated genes but is not a primary transcriptional activator of either. Mol Cell Biol 10:2448–2457. https://doi.org/10.1128/MCB.10.6.2448.
16. Harada H, Willison K, Sakakibara J, Miyamoto M, Fujita T, Taniguchi T. 1990. Absence of the type I IFN system in EC cells: transcriptional activator (IRF-1) and repressor (IRF-2) genes are developmentally regulated. Cell 63:303–312. https://doi.org/10.1016/0092-8674(90)90163-9.
17. Saha B, Jyothi Prasanna S, Chandrasekar B, Nandi D. 2010. Gene modulation and immunoregulatory roles of interferon gamma. Cytokine 50:1–14. https://doi.org/10.1016/j.cyto.2009.11.021.
18. Kimura T, Nakayama K, Penninger J, Kitagawa M, Harada H, Matsuyama T, Tanaka N, Kamijo R, Vilcek J, Mak TW. 1994. Involvement of the IRF-1 transcription factor in antiviral responses to interferons. Science 264:1921–1924. https://doi.org/10.1126/science.8009222.
19. Kollet JI, Petro TM. 2006. IRF-1 and NF-kappaB p50/cRel bind to distinct regions of the proximal murine IL-12 p35 promoter during costimulation with IFN-gamma and LPS. Mol Immunol 43:623–633. https://doi.org/10.1016/j.molimm.2005.04.004.
20. Liu J, Cao S, Herman LM, Ma X. 2003. Differential regulation of interleukin (IL)-12 p35 and p40 gene expression and interferon (IFN)-gamma-primed IL-12 production by IFN regulatory factor 1. J Exp Med 198:1265–1276. https://doi.org/10.1084/jem.20030026.
21. Liu J, Guan X, Ma X. 2005. Interferon regulatory factor 1 is an essential and direct transcriptional activator for interferon γ-induced RANTES/CCl5 expression in macrophages. J Biol Chem 280:24347–24355. https://doi.org/10.1074/jbc.M500973200.
22. Vila-del Sol V, Punzon C, Fresno M. 2008. IFN-gamma-induced TNF-alpha expression is regulated by interferon regulatory factors 1 and 8 in mouse macrophages. J Immunol 181:4461–4470. https://doi.org/10.4049/jimmunol.181.7.4461.
23. Kanazawa N, Kurosaki M, Sakamoto N, Enomoto N, Itsui Y, Yamashiro T, Tanabe Y, Maekawa S, Nakagawa M, Chen CH, Kakinuma S, Oshima S, Nakamura T, Kato T, Wakita T, Watanabe M. 2004. Regulation of hepatitis C virus replication by interferon regulatory factor 1. J Virol 78:9713–9720. https://doi.org/10.1128/JVI.78.18.9713-9720.2004.
24. Au WC, Raj NB, Pine R, Pitha PM. 1992. Distinct activation of murine interferon-alpha promoter region by IRF-1/ISFG-2 and virus infection. Nucleic Acids Res 20:2877–2884. https://doi.org/10.1093/nar/20.11.2877.
25. Schoggins JW, Rice CM. 2011. Interferon-stimulated genes and their antiviral effector functions. Curr Opin Virol 1:519–525. https://doi.org/10.1016/j.coviro.2011.10.008.
26. Brien JD, Daffis S, Lazear HM, Cho H, Suthar MS, Gale M, Jr, Diamond MS. 2011. Interferon regulatory factor-1 (IRF-1) shapes both innate and CD8(+) T cell immune responses against West Nile virus infection. PLoS Pathog 7:e1002230. https://doi.org/10.1371/journal.ppat.1002230.
27. Maloney NS, Thackray LB, Goel G, Hwang S, Duan E, Vachharajani P, Xavier R, Virgin HW. 2012. Essential cell-autonomous role for interferon (IFN) regulatory factor 1 in IFN-gamma-mediated inhibition of norovirus replication in macrophages. J Virol 86:12655–12664. https://doi.org/10.1128/JVI.01564-12.
28. Stirnweiss A, Ksienzyk A, Klages K, Rand U, Grashoff M, Hauser H, Kroger A. 2010. IFN regulatory factor-1 bypasses IFN-mediated antiviral effects through viperin gene induction. J Immunol 184:5179–5185. https://doi.org/10.4049/jimmunol.0902264.
29. Nandakumar R, Finsterbusch K, Lipps C, Neumann B, Grashoff M, Nair S, Hochnadel I, Lienenklaus S, Wappler I, Steinmann E, Hauser H, Pietschmann T, Kroger A. 2013. Hepatitis C virus replication in mouse cells is restricted by IFN-dependent and -independent mechanisms. Gastroenterology 145:1414–1423. https://doi.org/10.1053/j.gastro.2013.08.037.
30. Matsuyama T, Kimura T, Kitagawa M, Pfeffer K, Kawakami T, Watanabe N, Kundig TM, Amakawa R, Kishihara K, Wakeham A, Potter J, Furlonger CL, Narendran A, Suzuki H, Ohashi PS, Paige CJ, Taniguchi T, Mak TW. 1993. Targeted disruption of IRF-1 or IRF-2 results in abnormal type I IFN gene induction and aberrant lymphocyte development. Cell 75:83–97. https://doi.org/10.1016/S0092-8674(05)80086-8.
31. Ogasawara K, Hida S, Azimi N, Tagaya Y, Sato T, Yokochi-Fukuda T, Waldmann TA, Taniguchi T, Taki S. 1998. Requirement for IRF-1 in the microenvironment supporting development of natural killer cells. Nature 391:700–703. https://doi.org/10.1038/35636.
32. Lohoff M, Ferrick D, Mittrucker HW, Duncan GS, Bischof S, Rollinghoff M, Mak TW. 1997. Interferon regulatory factor-1 is required for a T helper 1 immune response in vivo. Immunity 6:681–689. https://doi.org/10.1016/S1074-7613(00)80444-6.
33. Nair S, Michaelsen-Preusse K, Finsterbusch K, Stegemann-Koniszewski S, Bruder D, Grashoff M, Korte M, Koster M, Kalinke U, Hauser H, Kroger A. 2014. Interferon regulatory factor-1 protects from fatal neurotropic infection with vesicular stomatitis virus by specific inhibition of viral replication in neurons. PLoS Pathog 10:e1003999. https://doi.org/10.1371/journal.ppat.1003999.
34. Miyamoto M, Fujita T, Kimura Y, Maruyama M, Harada H, Sudo Y, Miyata T, Taniguchi T. 1988. Regulated expression of a gene encoding a nuclear factor, IRF-1, that specifically binds to IFN-beta gene regulatory elements. Cell 54:903–913. https://doi.org/10.1016/S0092-8674(88)91307-4.
35. Odendall C, Kagan JC. 2015. The unique regulation and functions of type III interferons in antiviral immunity. Curr Opin Virol 12:47–52. https://doi.org/10.1016/j.coviro.2015.02.003.
36. Teo TH, Lum FM, Claser C, Lulla V, Lulla A, Merits A, Renia L, Ng LF. 2013. A pathogenic role for CD4+ T cells during Chikungunya virus infection in mice. J Immunol 190:259–269. https://doi.org/10.4049/jimmunol.1202177.
37. Calderon B, Suri A, Pan XO, Mills JC, Unanue ER. 2008. IFN-gamma-dependent regulatory circuits in immune inflammation highlighted in diabetes. J Immunol 181:6964–6974. https://doi.org/10.4049/jimmunol.181.10.6964.
38. Morrison TE, Whitmore AC, Shabman RS, Lidbury BA, Mahalingam S, Heise MT. 2006. Characterization of Ross River virus tropism and virus-induced inflammation in a mouse model of viral arthritis and myositis. J Virol 80:737–749. https://doi.org/10.1128/JVI.80.2.737-749.2006.
39. Robertson SJ, Lubick KJ, Freedman BA, Carmody AB, Best SM. 2014. Tick-borne flaviviruses antagonize both IRF-1 and type I IFN signaling to inhibit dendritic cell function. J Immunol 192:2744–2755. https://doi.org/10.4049/jimmunol.1302110.
40. Schoggins JW, Wilson SJ, Panis M, Murphy MY, Jones CT, Bieniasz P, Rice CM. 2011. A diverse range of gene products are effectors of the type I interferon antiviral response. Nature 472:481–485. https://doi.org/10.1038/nature09907.
41. Grieder FB, Vogel SN. 1999. Role of interferon and interferon regulatory factors in early protection against Venezuelan equine encephalitis virus infection. Virology 257:106–118. https://doi.org/10.1006/viro.1999.9662.
42. Muller U, Steinhoff U, Reis LF, Hemmi S, Pavlovic J, Zinkernagel RM, Aguet M. 1994. Functional role of type I and type II interferons in antiviral defense. Science 264:1918–1921. https://doi.org/10.1126/science.8009221.
43. Ank N, Iversen MB, Bartholdy C, Staeheli P, Hartmann R, Jensen UB, Dagnaes-Hansen F, Thomsen AR, Chen Z, Haugen H, Klucher K, Paludan SR. 2008. An important role for type III interferon (IFN-lambda/IL-28) in TLR-induced antiviral activity. J Immunol 180:2474–2485. https://doi.org/10.4049/jimmunol.180.4.2474.
44. Lazear HM, Nice TJ, Diamond MS. 2015. Interferon-lambda: immune

functions at barrier surfaces and beyond. Immunity 43:15–28. https://doi.org/10.1016/j.immuni.2015.07.001.
45. Yin J, Gardner CL, Burke CW, Ryman KD, Klimstra WB. 2009. Similarities and differences in antagonism of neuron alpha/beta interferon responses by Venezuelan equine encephalitis and Sindbis alphaviruses. J Virol 83:10036–10047. https://doi.org/10.1128/JVI.01209-09.
46. White LK, Sali T, Alvarado D, Gatti E, Pierre P, Streblow D, Defilippis VR. 2011. Chikungunya virus induces IPS-1-dependent innate immune activation and protein kinase R-independent translational shutoff. J Virol 85:606–620. https://doi.org/10.1128/JVI.00767-10.
47. Hyde JL, Gardner CL, Kimura T, White JP, Liu G, Trobaugh DW, Huang C, Tonelli M, Paessler S, Takeda K, Klimstra WB, Amarasinghe GK, Diamond MS. 2014. A viral RNA structural element alters host recognition of nonself RNA. Science 343:783–787. https://doi.org/10.1126/science.1248465.
48. Pine R. 1992. Constitutive expression of an ISGF2/IRF1 transgene leads to interferon-independent activation of interferon-inducible genes and resistance to virus infection. J Virol 66:4470–4478.
49. Cho H, Proll SC, Szretter KJ, Katze MG, Gale M, Jr, Diamond MS. 2013. Differential innate immune response programs in neuronal subtypes determine susceptibility to infection in the brain by positive-stranded RNA viruses. Nat Med 19:458–464. https://doi.org/10.1038/nm.3108.
50. Fox JM, Diamond MS. 2016. Immune-mediated protection and pathogenesis of chikungunya virus. J Immunol 197:4210–4218. https://doi.org/10.4049/jimmunol.1601426.
51. Morrison TE, Oko L, Montgomery SA, Whitmore AC, Lotstein AR, Gunn BM, Elmore SA, Heise MT. 2011. A mouse model of chikungunya virus-induced musculoskeletal inflammatory disease: evidence of arthritis, tenosynovitis, myositis, and persistence. Am J Pathol 178:32–40. https://doi.org/10.1016/j.ajpath.2010.11.018.
52. Hawman DW, Stoermer KA, Montgomery SA, Pal P, Oko L, Diamond MS, Morrison TE. 2013. Chronic joint disease caused by persistent chikungunya virus infection is controlled by the adaptive immune response. J Virol 87:13878–13888. https://doi.org/10.1128/JVI.02666-13.
53. Gardner J, Anraku I, Le TT, Larcher T, Major L, Roques P, Schroder WA, Higgs S, Suhrbier A. 2010. Chikungunya virus arthritis in adult wild-type mice. J Virol 84:8021–8032. https://doi.org/10.1128/JVI.02603-09.
54. Ziegler SA, Lu L, da Rosa AP, Xiao SY, Tesh RB. 2008. An animal model for studying the pathogenesis of chikungunya virus infection. Am J Trop Med Hyg 79:133–139.
55. Schilte C, Couderc T, Chretien F, Sourisseau M, Gangneux N, Guivel-Benhassine F, Kraxner A, Tschopp J, Higgs S, Michault A, Arenzana-Seisdedos F, Colonna M, Peduto L, Schwartz O, Lecuit M, Albert ML. 2010. Type I IFN controls chikungunya virus via its action on nonhematopoietic cells. J Exp Med 207:429–442. https://doi.org/10.1084/jem.20090851.
56. Noret M, Herrero L, Rulli N, Rolph M, Smith PN, Li RW, Roques P, Gras G, Mahalingam S. 2012. Interleukin 6, RANKL, and osteoprotegerin expression by chikungunya virus-infected human osteoblasts. J Infect Dis 206:455–457:457–459. https://doi.org/10.1093/infdis/jis368.
57. Schwartz O, Albert ML. 2010. Biology and pathogenesis of chikungunya virus. Nat Rev Microbiol 8:491–500. https://doi.org/10.1038/nrmicro2368.
58. Paquet C, Quatresous I, Solet JL, Sissoko D, Renault P, Pierre V, Cordel H, Lassalle C, Thiria J, Zeller H, Schuffnecker I. 2006. Chikungunya outbreak in Reunion: epidemiology and surveillance, 2005 to early January 2006. Euro Surveill 11(5):pii=2891. http://www.eurosurveillance.org/ViewArticle.aspx?ArticleId=2891.
59. Ozden S, Huerre M, Riviere JP, Coffey LL, Afonso PV, Mouly V, de Monredon J, Roger JC, El Amrani M, Yvin JL, Jaffar MC, Frenkiel MP, Sourisseau M, Schwartz O, Butler-Browne G, Despres P, Gessain A, Ceccaldi PE. 2007. Human muscle satellite cells as targets of Chikungunya virus infection. PLoS One 2:e527. https://doi.org/10.1371/journal.pone.0000527.
60. Poo YS, Nakaya H, Gardner J, Larcher T, Schroder WA, Le TT, Major LD, Suhrbier A. 2014. CCR2 deficiency promotes exacerbated chronic erosive neutrophil-dominated chikungunya virus arthritis. J Virol 88:6862–6872. https://doi.org/10.1128/JVI.03364-13.
61. Stoermer KA, Burrack A, Oko L, Montgomery SA, Borst LB, Gill RG, Morrison TE. 2012. Genetic ablation of arginase 1 in macrophages and neutrophils enhances clearance of an arthritogenic alphavirus. J Immunol 189:4047–4059. https://doi.org/10.4049/jimmunol.1201240.
62. Lucas-Hourani M, Dauzonne D, Jorda P, Cousin G, Lupan A, Helynck O, Caignard G, Janvier G, Andre-Leroux G, Khiar S, Escriou N, Despres P, Jacob Y, Munier-Lehmann H, Tangy F, Vidalain PO. 2013. Inhibition of pyrimidine biosynthesis pathway suppresses viral growth through innate immunity. PLoS Pathog 9:e1003678. https://doi.org/10.1371/journal.ppat.1003678.
63. Xu X, Williams JW, Shen J, Gong H, Yin DP, Blinder L, Elder RT, Sankary H, Finnegan A, Chong AS. 1998. In vitro and in vivo mechanisms of action of the antiproliferative and immunosuppressive agent, brequinar sodium. J Immunol 160:846–853.
64. Morris RE. 1995. Mechanisms of action of new immunosuppressive drugs. Ther Drug Monit 17:564–569. https://doi.org/10.1097/00007691-199512000-00003.
65. Tsetsarkin K, Higgs S, McGee CE, De Lamballerie X, Charrel RN, Vanlandingham DL. 2006. Infectious clones of Chikungunya virus (La Reunion isolate) for vector competence studies. Vector Borne Zoonotic Dis 6:325–337. https://doi.org/10.1089/vbz.2006.6.325.
66. Pal P, Dowd KA, Brien JD, Edeling MA, Gorlatov S, Johnson S, Lee I, Akahata W, Nabel GJ, Richter MK, Smit JM, Fremont DH, Pierson TC, Heise MT, Diamond MS. 2013. Development of a highly protective combination monoclonal antibody therapy against Chikungunya virus. PLoS Pathog 9:e1003312. https://doi.org/10.1371/journal.ppat.1003312.
67. Tanaka N, Ishihara M, Kitagawa M, Harada H, Kimura T, Matsuyama T, Lamphier MS, Aizawa S, Mak TW, Taniguchi T. 1994. Cellular commitment to oncogene-induced transformation or apoptosis is dependent on the transcription factor IRF-1. Cell 77:829–839. https://doi.org/10.1016/0092-8674(94)90132-5.
68. Schluter D, Kwok LY, Lutjen S, Soltek S, Hoffmann S, Korner H, Deckert M. 2003. Both lymphotoxin-alpha and TNF are crucial for control of Toxoplasma gondii in the central nervous system. J Immunol 170:6172–6182. https://doi.org/10.4049/jimmunol.170.12.6172.
69. Fox JM, Long F, Edeling MA, Lin H, van Duijl-Richter MK, Fong RH, Kahle KM, Smit JM, Jin J, Simmons G, Doranz BJ, Crowe JE, Jr, Fremont DH, Rossmann MG, Diamond MS. 2015. Broadly neutralizing alphavirus antibodies bind an epitope on E2 and inhibit entry and egress. Cell 163:1095–1107. https://doi.org/10.1016/j.cell.2015.10.050.